Aalto University

OPEN ACCESS

This is an electronic reprint of the original article.
This reprint may differ from the original in pagination and typographic detail.

Peng, Chao; Lahtinen, Katja; Medina, Elena; Kauranen, Pertti; Karppinen, Maarit; Kallio, Tanja; Wilson, Benjamin P.; Lundström, Mari

Role of impurity copper in Li-ion battery recycling to $LiCoO_2$ cathode materials

Published in:
Journal of Power Sources

DOI:
10.1016/j.jpowsour.2019.227630

Published: 29/02/2020

Document Version
Publisher's PDF, also known as Version of record

Published under the following license:
CC BY-NC-ND

Please cite the original version:
Peng, C., Lahtinen, K., Medina, E., Kauranen, P., Karppinen, M., Kallio, T., Wilson, B. P., & Lundström, M. (2020). Role of impurity copper in Li-ion battery recycling to $LiCoO_2$ cathode materials. *Journal of Power Sources*, *450*, Article 227630. https://doi.org/10.1016/j.jpowsour.2019.227630

This material is protected by copyright and other intellectual property rights, and duplication or sale of all or part of any of the repository collections is not permitted, except that material may be duplicated by you for your research use or educational purposes in electronic or print form. You must obtain permission for any other use. Electronic or print copies may not be offered, whether for sale or otherwise to anyone who is not an authorised user.

Journal of Power Sources 450 (2020) 227630

Contents lists available at ScienceDirect

Journal of Power Sources

journal homepage: www.elsevier.com/locate/jpowsour

Role of impurity copper in Li-ion battery recycling to $LiCoO_2$ cathode materials

Chao Peng [a], Katja Lahtinen [b], Elena Medina [b], Pertti Kauranen [b], Maarit Karppinen [b], Tanja Kallio [b], Benjamin P. Wilson [a], Mari Lundström [a,*]

[a] *Department of Chemical and Metallurgical Engineering (CMET), Aalto University, School of Chemical Engineering, 02150, Espoo, Finland*
[b] *Department of Chemistry and Materials Science (CMAT), Aalto University, School of Chemical Engineering, 02150, Espoo, Finland*

HIGHLIGHTS

- Behavior of Li, Co and Cu during the recycling of LIBs waste was investigated.
- Cu-contaminated LCOs were synthesized with the recycled Co and Li products.
- Cu contamination induced up to ca. 35 mAh/g decrease in initial specific capacity.
- Cu contamination could enhance the conductivity and cyclability of the recycled LCO.
- Cu contamination improves the specific capacity at high discharge rates.

ARTICLE INFO

Keywords:
Waste Li-ion batteries
Hydrometallurgy
Closed-loop approach
Positive electrode
Electrochemical performance

ABSTRACT

Copper is a dominating impurity in Co-rich $Li(Co,Ni,Mn)O_2$ battery waste fractions and may exist in similar quantities (e.g. 6 wt%) as Li, Ni and Mn. This paper investigates the behavior of copper from waste batteries up to recycled active materials and the findings highlight that copper contamination is not necessarily detrimental for the active materials in trace amounts, but can rather increase the discharge capacity at high rates. Firstly, industrially crushed battery waste was treated hydrometallurgically to produce Li_2CO_3 and $CoSO_4{\cdot}2H_2O$ precipitates for re-use, before being calcined to prepare fresh $LiCoO_2$ materials. Results suggest that during the hydrometallurgical recycling process, Cu is likely to co-extract along the Co; in the current work both high and low Cu-contaminated $CoSO_4{\cdot}2H_2O$ precipitates were obtained and in the former case, formation of CuO as a secondary phase occurred upon calcination. The presence of Cu contamination induced up to ca. 35 mAh/g decrease in the specific capacity, compared to pure $LiCoO_2$. However, a low level of Cu inclusion was found to be advantageous at high discharge rates (4.0C and 5.0C) resulting in a doubling of the capacity (110–120 mAh/g) when compared with pure $LiCoO_2$ (40–60 mAh/g).

1. Introduction

Li-ion batteries (LIBs) have been extensively utilized in consumer electronics, electric vehicles and energy storing devices because of their high voltage, high energy density, low self-discharge and lack of memory effect, etc. [1]. The consumption of LIBs has increased by nearly 20 times in the last two decades, from 500 million units in 2000 to an expected level of 10 billion in 2020, resulting in a large amount of end-of-life spent LIBs [2]. Statistics show that the generation of spent LIBs from electric vehicles in China was almost 10,000 tons in 2016 and this amount is expected to continue to grow rapidly in the future [3]. These spent LIBs are considered to be significant secondary raw material resources as they contain ca. 5–30 wt% Co, 0–10 wt% Ni, 2–12 wt% Li, 7–17 wt% Cu, 3–10 wt% Al, 0–25 wt% Fe as well as some graphite [4]. In addition, there may be safety or environmental risks related to e.g. the toxic and flammable electrolytes contained within the battery matrix. Therefore, in order to protect the environment and avoid the waste of resources, recycling of the spent LIBs has recently attracted a lot of attention.

Nevertheless, it has been estimated that currently only <1% of Li is recycled by state-of-art operators [5,6], although a more recent report suggests that this may be an under-estimation [7]. When subjected to

---

* Corresponding author.
E-mail address: mari.lundstrom@aalto.fi (M. Lundström).

https://doi.org/10.1016/j.jpowsour.2019.227630
Received 28 August 2019; Received in revised form 26 November 2019; Accepted 16 December 2019
Available online 25 December 2019
0378-7753/© 2019 The Authors. Published by Elsevier B.V. This is an open access article under the CC BY-NC-ND license (http://creativecommons.org/licenses/by-nc-nd/4.0/).

recycling, the waste LIBs scraps can be treated by several different mechanical, pyrometallurgical, hydrometallurgical and biological methods, which have been reviewed in several scientific papers [8–10]. In particular, hydrometallurgical techniques can offer a promising alternative for the sustainable recycling of spent batteries in future. A typical hydrometallurgical recycling process for waste LIBs usually involves acid leaching, followed by subsequent purification and recovery steps like precipitation, solvent extraction and adsorption [11–14]. Literature suggest, for example, that over 95% of Co and Li can be leached out with a sulfuric acid based system in the presence of excess H_2O_2 [15,16]. Of this, 95–98% of Co can be recovered and separated from Li and Ni in acid leaching solution by 0.4 M Bis(2,4,4-trimethylpentyl)-phosphinic acid (Cynaex 272) at pH 5.5–6.0 [17] and 85–90% Li is recoverable as Li_2CO_3 by carbonation [18].

Although many of the published works have focused on the recovery of Co and Li, this is often from synthetic solutions or from active material fractions that rarely represent the real industrial battery waste. In reality, state-of-the-art processes include fractions that not only contain active materials, but also impurities such as Al, Cu, Fe etc. which originate from the current collector materials and the outer cases of batteries. The interaction of impurities with the active battery metals in each step of the battery waste recycling value chain (pre-treatment, hydrometallurgical processing, recovery, calcination and cycling processes) has both a metallurgical and an electrochemical impact on the recycled battery materials. For instance, high losses of metals (e.g. 52% Ni and 38% Co) have been reported during the removal of Fe and Al by neutralization and precipitation at pH 6.8 [19]. In addition, complete separation of Cu from other active battery metals such as Co, Mn and Ni is also very challenging, as it usually involves multi-stage solvent extraction process that required expensive Cu-specific extractants (e.g. Acorga M 5640) [20]. Consequently, the total recovery of Co and Li from the real industrially crushed raw materials, in practice, has not been high – e.g. Li recoveries as low as 60–80% are commonly reported [6]. In addition, impurities that originate from the crushed raw material can easily contaminate the final recycled products.

The effect of different impurities within electrode materials on their electrochemical properties has been investigated in detail through the use of dopants. Generally, small amounts of other metals, such as Mg, Ti, Zr, Mn, Fe, Ni, Cu, Zn and Al, can enhance the properties of layered metal oxides like $LiCoO_2$ and $LiNi_xMn_yCo_{1-x-y}O_2$ ($x,y < 1$) [21,22]. The present of dopant can, for example, enhance the material conductivity or stabilize the crystal structure thus enhancing the cyclability of the active material. However, in many cases the introduction of an electrochemically inactive element decreases the reversible capacity, even if the stability of the material is enhanced.

Copper doping in $LiCoO_2$ has been investigated previously in several studies [23,24], whereas dual-doping of $LiCoO_2$, in which Cu is one of the dopants, has also been investigated [25,26]. Kang et al. [27] reported that the lower valence of Cu compared to that of Co lowers the Li migration barrier and therefore enhances Li diffusion in the material. This is consistent with the study by Nityha et al. [24] that showed enhanced capacities for $LiCoO_2$ and enhanced stability – an upper voltage limit as high as 4.6 V was found to be achievable - with Cu doping. A possible drawback to the usage of Cu as a dopant is its potential dissolution and migration to the negative electrode in full cells, where it can subsequently be reduced to metallic copper resulting in a safety risk. Nevertheless, previous research by Kim et al. [23] found no evidence of this type of behavior in pouch cells, although it should be noted that the particles investigated were carefully engineered to have an egg-shell type of structure, which could be beneficial when compared to the conventional doping.

In this study, the input LIBs waste is mechanically pretreated using an industrial process and the raw material consists of both active material (containing Li, Co, Ni, Mn) and other 'impurity elements' like Al, Fe, and Cu. The multi-metal matrix behavior of all these metals is investigated with the primary focus on copper as the main impurity metal. Moreover, the possible losses of Co and Li at each step from the acid leaching through purification to the production of the Li_2CO_3 and $CoSO_4$ products are also studied. The flowsheet for the recovery of Li and Co is based on known industrial unit processes, which makes this paper relevant for the related industries, although only the optimum conditions for each step are studied [28–31]. Furthermore, $LiCoO_2$ (LCO) active material is synthesized from the recycled Li_2CO_3 and $CoSO_4$ products and the influence of the Cu contamination on the specific capacity and specific discharge capacity of the recycled $LiCoO_2$ is studied. According to the best of the authors' knowledge, this is the first time when such a closed-loop approach is conducted all the way from real recycled materials up to performance measurements of new active materials. The results presented provide a new understanding of the effect of impurities during closed-loop processing of Li-battery waste.

2. Experimental

2.1. Raw material: battery waste and the pregnant leach solution (PLS)

The portable waste LIBs were pretreated industrially by crushing, magnetic separation and sieving into < 2 mm fraction, by the procedure outlined earlier [32]. Table 1 shows that the battery waste fraction had a high content of Co (23.6 wt%), and that the second largest metallic element was Cu (6.2 wt%), although Li, Al and Ni were all also present in appreciable amounts (ca. ~3 wt%). Based on our previous hydrometallurgical research [29], the LIBs waste obtained was leached using 2 M H_2SO_4 and 5 vol% H_2O_2 with a liquid-to-solid (L/S) ratio of 10:1 (mL/g) at 75 °C for 1 h 100 g of scraps were treated and 1156 mL (containing the washing water solution) pregnant leaching solution (PLS1) was obtained. The chemical composition of the LIBs scraps input and PLS1 were determined by inductively coupled plasma-optical emission spectroscopy (ICP-OES, PerkinElmer Optima 7100 DV, USA). This hydrometallurgical procedure allows partial Cu reduction during the leaching and therefore in PLS1 the copper does not tend to predominate over Li, Al and Ni (Table 1). Leaching extraction of Co and Li were determined to be up to ca. 98% whereas ca. 69% of Cu was also dissolved.

2.2. Experimental procedures

2.2.1. Recovery of Li_2CO_3 and $CoSO_4$ from the PLS

The obtained PLS1 rich in valuable metals and impurities (Li, Co, Ni, Mn, Cu, Fe and Al) was subjected to a series of unit processes to recover Co and Li, which involved Fe and Al removal by Di-(2-ethylhexyl) phosphoric acid (D2EHPA) resulting in PLS2, Cu removal by precipitation (PLS3) and Co recovery by Cynaex 272, followed by stripping and $CoSO_4$ crystallization (Batch 1 and Batch 2). The Co free solution (PLS4) was then subjected to Ni removal by precipitation - to produce PLS5 - from which, Li was recovered as Li_2CO_3 by carbonation and evaporation. The operating parameters of each step are presented in Table 2.

It is worth noting that in order to simulate the last stages of counter-current Co extraction by Cynaex 272 in industry, the same aqueous solution (PLS3) was contacted with fresh organic solvent 5 times at pH ca. 5.0 in order to reduce the target element (Co) in the aqueous solution. As a result, five batches of loaded organic solution were produced and the first two batches of organic solutions that should contain higher levels of impurities (e.g. Cu, Mn) were mixed and in order to produce the first cobalt salt batch (1# $CoSO_4$) by stripping, evaporation and crystallization. The second batch (2# $CoSO_4$) was produced by mixing of the

Table 1
The composition and concentration of metals in LIBs scraps and pregnant leaching solution.

Elements	Cu	Mn	Fe	Ni	Co	Li	Al
LIBs scraps (%)	6.2	1.7	0.7	2.7	23.6	3.7	2.8
PLS1 (g/L)	3.7	1.5	0.6	2.4	19.7	3.5	2.4

Table 2
Operating parameters in the unit processes used to recover Co and Li from the initial leaching solution (PLS1).

Process	Product	Operating parameters
Fe, Al removal	PLS2	3-Stage cross current SX process: O:A = 1:1, 15 vol% D2EHPA + 5 vol% TBP, pH = 2.5–3.0
Cu separation	PLS3	Precipitation: pH = 5.20, 25 °C
Co extraction	PLS4+ Co sol[a]	5-stage cross current SX process: 15 vol% Cyanex 272, pH = 4.70–5.20, O:A = 1:1, 25 °C
Co recovery	*1# $CoSO_4$* *2# $CoSO_4$*	Evaporation (boiling) and crystallization (room temperature)
Ni separation	PLS5	Precipitation: pH = 12.5, 25 °C
Li recovery	*Li_2CO_3*	Evaporation and carbonation: Na_2CO_3:Li^+ = 0.6:1 (mol ratio), 90 °C, 30 min.

[a] Refers to Co rich stripping solution obtained from the organic phase.

three remaining loaded organic solutions that contained less impurities. The overall mass balance of metals (Co, Li, Cu) after each process step were calculate based upon the concentration of the resultant PLS, via equation (1):

$$\gamma_i = (C_i \times V)/(m_o \times w_o) \times 100\% \tag{1}$$

where $m_i(g)$ and $w_i(\%)$ are the mass of the input materials and the chemical compositions of element (i), respectively; C_i and V_i are the concentration of element (i) and the volume of PLS.

2.2.2. Preparation of active materials by calcination

Before the synthesis of $LiCoO_2$ or LCO active electrode material from the recycled precursors, the recycled and precipitated cobalt salt (previously referred to as $CoSO_4$) was investigated using thermogravimetric analysis (TGA; PerkinElmer, Pyris 1 thermal balance, 25–950 °C, air atmosphere) to study the temperature stability of the sample and to determine the number of water molecules present in the structure (the n value in $CoSO_4{\cdot}nH_2O$). Due to the hygroscopic nature and therefore difficulties in the weighing procedure, the hydrated pink $CoSO_4{\cdot}nH_2O$ salt (Batch 1# and 2#) was heat treated in air at 700–950 °C for 12 h to remove water, sulfur and also to obtain black Co_3O_4, which was subsequently used in the LCO preparation process. The resultant recycled Co_3O_4 was mixed with the recycled Li_2CO_3 powder (in stoichiometric amounts) and the powder mixture was pelletized and heated in an alumina crucible in air at 800 °C for 24 h in order to conduct the final $LiCoO_2$ synthesis. For comparison, a reference $LiCoO_2$ sample was prepared by an identical procedure from pure virgin reactants Co_3O_4 (99.7%, Alfa Aesar) and Li_2CO_3 (99.0%, Alfa Aesar). The particle size and morphology of the investigated materials were studied with Scanning electron microscopy (SEM, Tescan Mira3, in-beam secondary electrons).

2.2.3. Electrochemical performance measurement

The samples for electrochemical tests were prepared as follows: A slurry with a consistency of 95 wt% of active material, 3 wt% polyvinylidene fluoride (PVDF, Solvay, Solef 5130) and 2 wt% carbon black (Timcal Super C65) was mixed in N-methyl-2-pyrrolidone (NMP, BASF, Life Science) with a dispersant (Dispermat, VMA-Getzmann GMBH-D-51580 Reichshof). The dry material content of the resultant slurry was 60 wt% and it was coated on an aluminum foil with a loading of 5.7–7.3 mg/cm^2 before being dried overnight in air. The coatings were then also subsequently dried in an oven at 80 °C for 4 h. Electrodes with diameter of 14 mm were cut and calandered with a pressure of 3250 $kg\ cm^{-2}$. The newly produced electrodes were then dried overnight at 110 °C in a vacuum oven, before being transferred to a glovebox with an argon atmospheric (Jacomex) and assembled into half-cells.

The active material electrode was utilized as the positive electrode in the cells. 0.75 mm thick lithium metal foil (Alfa Aesar) was used as counter electrode and 1 M LiPF6 in 1:1 ethylene carbonate (EC): dimethyl carbonate (DMC) as an electrolyte (BASF, LP30). Glass fiber filters (Whatman, GF/A, 0.26 mm) was used in the cells as the separator, along with MTI 0.2 mm spacers. In the last stage, the completed electrode materials were sealed inside Hohsen 2016 coin cells. After cell assembly, the coin cells were allowed to stabilize for 24 h prior to the commencement of the measurements.

The rate capabilities of the coin cells were measured with a Neware battery cycler using the following program: Initial formatting was performed with a C-rate of 0.03 C and then three cycles of 0.1 C. After this, the measurement was continued by maintaining the charging C-rate at 0.2 C but varying the discharge C-rate from 0.2 C through 0.5 C, 1.0 C, 2.0 C and 4.0 C–5.0 C and measuring three cycles per each C-rate. After this, three more 0.2 C cycles were performed to obtain tentative information about the cyclability properties of the materials. The voltage range was 3.0–4.3 V.

Electrochemical impedance spectroscopy (EIS) was performed over a frequency range of 10^5–10^{-2} Hz with a Metrohm Autolab PGSTAT302 N potentiostat and FRA program using EL-CELL ECC-Combi three-electrode cell setup and an amplitude of 5 mV. The EIS was measured after assembly, 20 cycles and 50 cycles with aging performed using a C-rate of 0.5C.

3. Results and discussion

3.1. Recovery of Li and Co from waste LIBs scraps

Table 3 shows the chemical compositions of the solutions obtained at each recycling process unit step (PLS1-5) and the prepared $CoSO_4$ and Li_2CO_3 products. It was found that the recycled $CoSO_4$ product suffers from impurity contamination that is dominated by Cu. Batch #1 had a high Cu contamination (Cu/Co ratio of 0.15), whereas batch #2 had a much lower level of Cu contamination (Cu/Co ratio of 0.02). This is attributed to the fact that: (i) not all Cu was removed in the Cu precipitation stage and (ii) Cu can be co-extracted along with the Cyanex 272 in the SX process presented. Nonetheless, results suggest that the stripping conditions did affect the level of contamination in the final Co product. In the current study, 68.7% of Cu was dissolved during the reductive leaching and of this, 64.1% of Cu was still in the solution at the start of the Cu removal stage. Although a majority of Cu was extracted during this process, PLS 3 was still found to contain 31.5% of the input copper. This all was extracted by Cyanex 272 together with Co, with Cu contamination levels of 12.6% (Batch #1) and 2.1% (Batch 2#) found in the $CoSO_4$ product. In contrast, it was found that the Li rich solution (PLS5) had almost no impurities and therefore a high-purity Li_2CO_3 product could be produced. The XRD patterns of the Li_2CO_3 product and two batches of $CoSO_4$ product are displayed in Fig. S1 and the results show that the Li_2CO_3 exists in its anhydrous form, whereas $CoSO_4$ products (Batch 1# and 2#) are in the form of $CoSO_4{\cdot}nH_2O$. Additionally, impurity peaks are either not visible in both Li_2CO_3 and $CoSO_4$ products or they are obscured by the peaks of the main phases.

The whole flowsheet with the mass balances of Co, Li and Cu are presented in Fig. 1. The results suggest that the direct Co and Li recovery is 52.8% and 54.6%, respectively. The low recovery of Co mainly results from the high loss of Co (ca. 35.4%) in the solution after crystallization of $CoSO_4$ products. Nevertheless, the Co-rich residual solution can be circulated back to the process (with PLS2) and then recycled in the subsequent process to give a total Co recovery of approximately 88.5%, which is close to previously reported results [33]. As for Li, nearly half is lost as follows: 12.0% in the solvent extraction, 16.6% in evaporation process and 13.6% in the carbonation process. The Li co-extracted with Co can be recovered by scrubbing the loaded organic phase with $CoSO_4$ solution in industrial production as has been reported before [31,33]. The high loss of Li in the evaporation process can be attributed to the

Table 3
Chemical compositions of solution samples and the produced Li_2CO_3 and $CoSO_4$ products.

Samples	Elements							
	Cu	Mn	Fe	Ni	Co	Li	Al	Na
PLS1 (g/L)	3.71	0.86	0.68	2.38	19.70	3.45	2.83	–
PLS2 (g/L)	3.46	0.63	0.01	2.31	20.27	3.46	0.25	–
PLS3 (g/L)	1.70	0.60	0.01	2.15	18.97	3.45	0.20	–
PLS4 (g/L)	0.00	0.01	0.01	1.86	0.66	2.92	0.03	–
PLS5 (g/L)	4.5×10^{-4}	9.5×10^{-4}	0.1×10^{-4}	2.4×10^{-3}	7.8×10^{-4}	2.90	1.8×10^{-3}	–
Li_2CO_3 (%)	<0.01	<0.01	<0.01	<0.01	<0.01	17.11	<0.01	0.29
$CoSO_4$ #1 (%)	3.53	1.85	0.01	0.01	23.48	0.02	0.01	0.03
$CoSO_4$ #2 (%)	0.51	0.43	<0.01	0.01	23.56	0.02	0.02	0.02

formation of $NaLiSO_4$, (see supporting materials).

3.2. Preparation of active materials

From TGA, the water content in the recycled $CoSO_4{\cdot}nH_2O$ was determined to be n = 4 (Fig. S3). In addition, it was revealed that the decomposition of $CoSO_4{\cdot}2H_2O$ to Co_3O_4 started around 750 °C in air.

Based upon these results, the water and sulfur removal from $CoSO_4{\cdot}2H_2O$ was first tested at T = 700–950 °C (Fig. S4) and from the results, the optimized calcination temperature was determined to be around 850 °C. Fig. 2 displays the XRD patterns for the Co_3O_4 powder obtained at 850 °C and the LCO ($LiCoO_2$) electrode material subsequently synthetized from the calcined Co_3O_4 and recycled Li_2CO_3. It can be seen that the Cu rich raw material (Batch #1) results in low levels of CuO formation, which can be identified both in the Co_3O_4 intermediate, as well as in the final LCO. On the other hand Batch #2, with significantly lower Cu contamination, does not any presence of CuO and the XRD pattern is essentially identical to that of reference LCO prepared from the pure virgin raw materials.

The SEM images of the synthesized LCO materials in Fig. 3 show that there are clear differences in the morphology of the Cu-rich and the low-Cu particles. The Cu-rich LCO material has an average particle size of 3.5 μm, whereas the low-Cu is 1.9 μm. In addition, the Cu-rich particles seem to consist of agglomerated primary particles while low-Cu particles do not. The virgin reference material has the largest average particle size of 4.9 μm and its morphology is similar to that of the Cu-rich material, i.e. primary particles agglomerate to form larger particle sizes.

Chemical composition of the impurities present in the LCO materials was determined by ICP-OES following digestion with aqua regia for 24 h. Results in Table 4 show that Cu-rich LCO materials derived from Batch #1 $CoSO_4{\cdot}2H_2O$, consist of 91.5 mg/g Cu, 46.2 mg/g Mn, as well as traces (<1 mg/g) of Fe, Ni, Al and Na. In contrast, the chemical composition of the impurities present within the low-Cu LCO produced from Batch #2 $CoSO_4$ product are much lower at 4.8 mg/g Cu and 3.3 mg/g Mn.

3.3. Electrochemical performance

Cu-rich LCO, low-Cu LCO and the reference LCO materials were compared for their electrochemical performance and the results are presented in Fig. 4. Cyclic voltammetry curves with peak separations of 53 mV (Cu-rich LCO), 68 mV (low-Cu LCO) and 102 mV (reference LCO) are shown in Fig. 4a and these results suggests that the resistance of the Cu-rich material is the lowest, whereas it is largest for the reference LCO. This is in line with previous studies that have shown that the presence of Cu can increase the Li diffusion within a sample [27]. The two small peaks detected for low-Cu LCO and the reference LCO at approximately 4.07 V and 4.18 V are caused by reversible Li ordering from rhombohedral symmetry to monoclinic symmetry [34,35] and such phase changes are indicative of good $LiCoO_2$ordering [36]. The same peaks are not observed in the Cu-rich LCO material, but as the ordering is disturbed by the presence of Cu and its content in the Cu-rich LCO is relatively high, this can be expected.

The rate capability results are presented in Fig. 4b, c and d. The initial capacities at the 0.03 C for the LCOs during charge and discharge were 166 mAh/g and 160 mAh/g (virgin reference), 148 mAh/g and 128 mAh/g (Cu-rich) and 163 mAh/g and 147 mAh/g (low-Cu). The specific discharge capacity of the reference is typical for $LiCoO_2$ within this voltage range, which suggests that the specific capacities of the investigated LCOs prepared from the recycled samples are lower than the typical specific capacities for pure LCO. For the Cu-rich sample, this is most likely caused by the electrochemically inactive copper within the material, whereas in the case of the low-Cu sample the lower discharge capacity results from the loss of Li during the initial charge. These Li losses can be most likely attributed to the smaller particle size observed in Fig. 3b, as the surface area reacting with the electrolyte is larger.

On the other hand, when the rate capability properties of the investigated samples are taken into consideration, it can be observed that the specific capacity of the recycled samples (Cu-rich and low-Cu LCOs) decreases much less with increasing C-rate when compared to the specific capacity of the reference LCO. At 1.0 C the specific capacity of the reference is still higher (138 mAh/g) while it is approximately 114 mAh/g for the Cu-rich and 131 mAh/g for the low-Cu LCO. Surprisingly, at 4.0 C the situation reverses, as the specific capacity of the recycled samples becomes comparatively larger (100 mAh/g for Cu-rich and 116 mAh/g for low-Cu LCO) than that of reference (87 mAh/g). This is a very promising result. In addition, if the initial 0.2 C capacities and the final 0.2 C capacities are compared, the capacity drop is smaller for the recycled materials than it is for the reference, which indicates an enhanced cyclability for the recycled materials. It should also be noted that the over-potential is higher for the final cycle of the reference material, as is seen when the charge-discharge curve separations in Fig. 4d are compared. This, along with the better rate capabilities of the Cu-rich and low-Cu LCOs suggests that the conductivity of the Cu-contaminated LCOs is better, most likely as a consequence of the presence of the Cu impurity. These findings were also confirmed by the EIS experiments presented in Fig. 5.

Nyquist plots of the investigated materials consist of two semicircles at the high and mid-frequencies, and additionally, the non-aged cells also show a diffusion tail at low frequencies. The smaller semicircle at the high frequencies is typically attributed to the interfacial contacts within the electrode, such as the passivation layer on top of the active material or the electrode-current collector interface. The second semicircle comes from the charge transfer resistance of the electrode material [37,38]. The cycling results presented in Fig. 5b show that both the recycled materials investigated, Low-Cu and Cu-rich LCOs, provide enhanced cyclability *cf.* reference LCO. This correlates with the observations from the rate capability results when the initial and final 0.2 C capacities are compared. The capacity drop of the reference is ascribed to the large increase in the charge transfer resistance observed during the cycling. Of all the materials investigated, the Cu-rich LCO shows the best cyclability, which is probably due to not only the Cu in the sample but also the low level of Mn - typically used as a stabilizing dopant in lithium metal oxide electrode materials - also present as indicated by the ICP-OES results (Table 4). Surprisingly, the charge transfer resistance increase is larger for the Cu-rich material than it is for the low-Cu

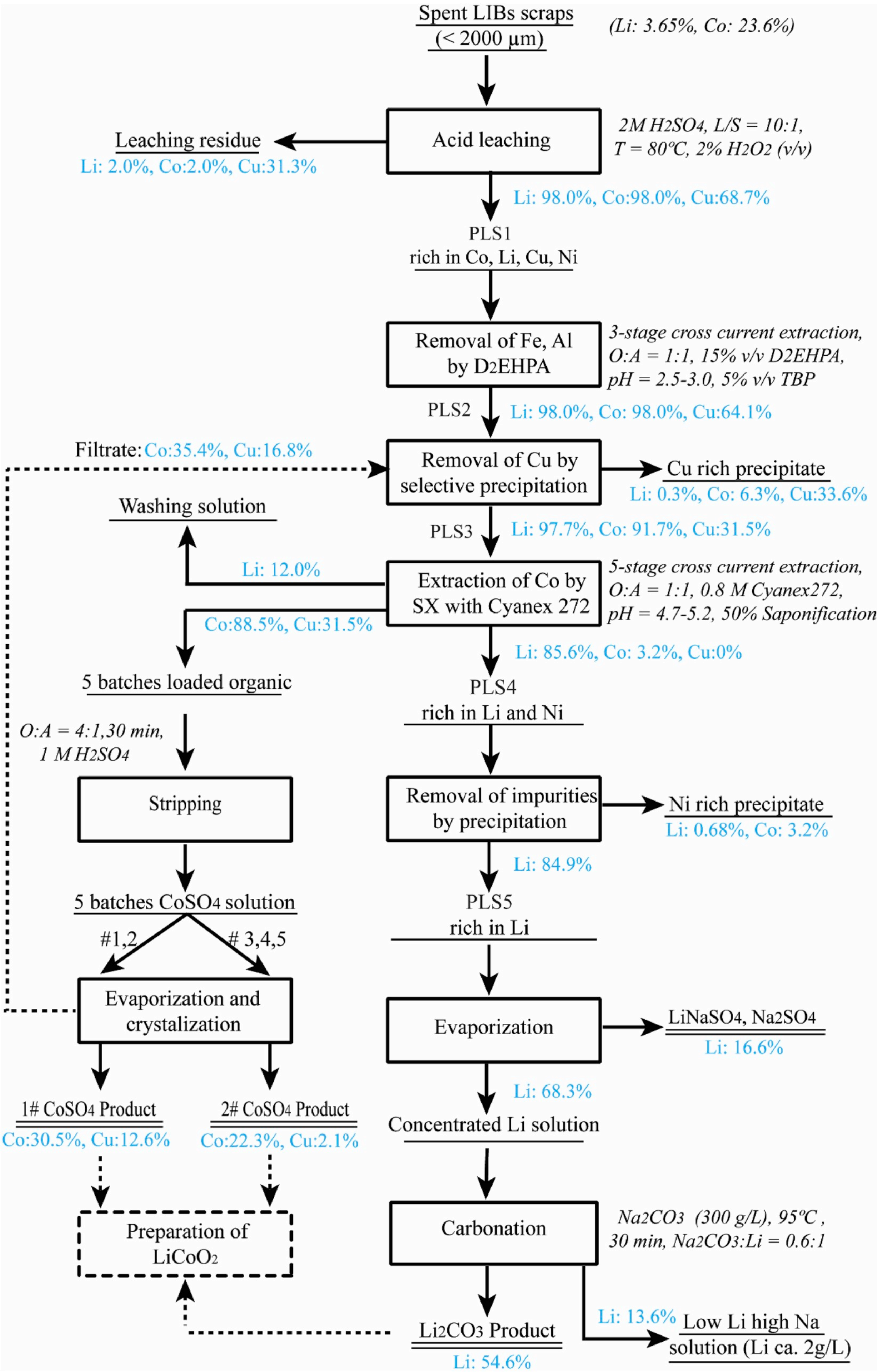

Fig. 1. Flowsheet for the preparation of Li_2CO_3 and $CoSO_4$ from leaching solution. The blue color shows the distribution of the elements into the fractions. (For interpretation of the references to color in this figure legend, the reader is referred to the Web version of this article.)

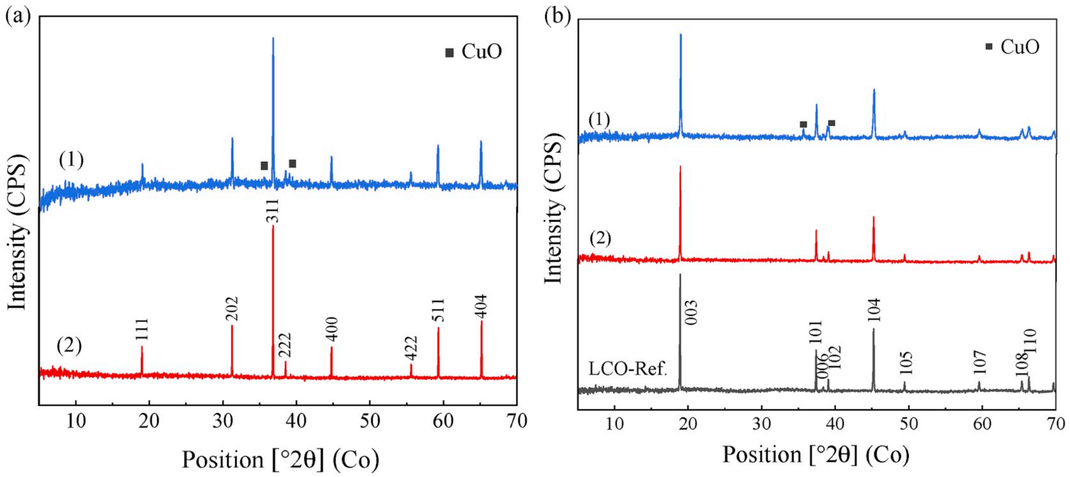

Fig. 2. XRD patterns of (a) Co_3O_4 and (b) final LCO powders obtained from Batch #1 Cu-rich (1) and Batch #2 low-Cu (2) $CoSO_4 \cdot 2H_2O$.

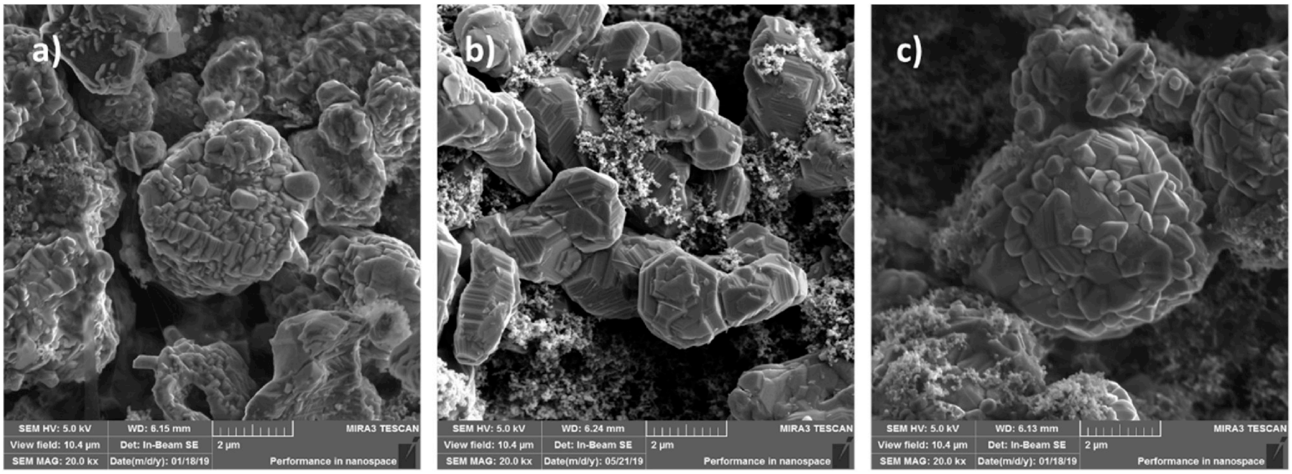

Fig. 3. The SEM images of the synthesized active materials, a) recycled Cu-rich LCO, b) recycled low-Cu LCO and c) virgin reference LCO.

Table 4
Impurities present in the prepared LCO active materials.

Samples	Impurity elements (mg/g)					
	Cu	Mn	Fe	Ni	Al	Na
Cu-rich LCO	91.5	46.2	0.35	0.25	0.34	0.99
Low-Cu LCO	4.8	3.3	0.67	0.29	0.22	0.16

material, however, as can be observed in Fig. 5d, the high-frequency semicircle of the Cu-rich material is smaller than that of the low-Cu material. Therefore, the reason for the good cyclability of Cu-rich LCO seems to be the enhanced electrode-current collector interphase resistance. The larger high-frequency semicircle of the low-Cu LCO also proves that the capacity drop between the initial charge and discharge cycles observed in Fig. 2b is caused by the increased electrolyte reaction at the particle surface due to a smaller particle size.

4. Discussion

Based on the electrochemical results, it is clear that Cu-rich LCO has a lower specific discharge capacity when compared to the reference LCO prepared from virgin materials. The specific discharge capacity of the low-Cu LCO is higher than that of the Cu-rich sample, but is still lower than that of the reference LCO although, the stability of the Cu-rich and low-Cu LCOs are better. Nevertheless, it should be considered that the copper in the positive electrode could have dissolved and then precipitated in the negative electrode. In the case of half-cells, where the metallic lithium acts as a counter electrode, the presence of metallic copper does not necessarily cause problems. In contrast, with a full cell configuration, metallic copper could cause problems, therefore further research with long-term cycling should be carried out.

Moreover, it is evident that both the battery recycling processes as well as the use of recycled battery materials in new battery applications should be investigated further. As recycling processes have numerous variations in their configuration and performance, there is therefore a reciprocal accumulation of different impurities within the final products. Although some of these impurities may even be beneficial, for the operational convenience state-of-the-art industrial processes target the production of extremely high purity metallic salts that can be subsequently doped by minor elements in the active material preparation phase. Nonetheless, the presence of contamination of elements like Ni, Mn, etc. in the salts used in LMO preparation are not necessarily a disadvantage and may even become a reason for the non-complete separation of target metals in future recycling processes.

5. Conclusion

The objective of this investigation was to study the behavior of Li, Co and Cu - as the main impurity - in the hydrometallurgical recycling of

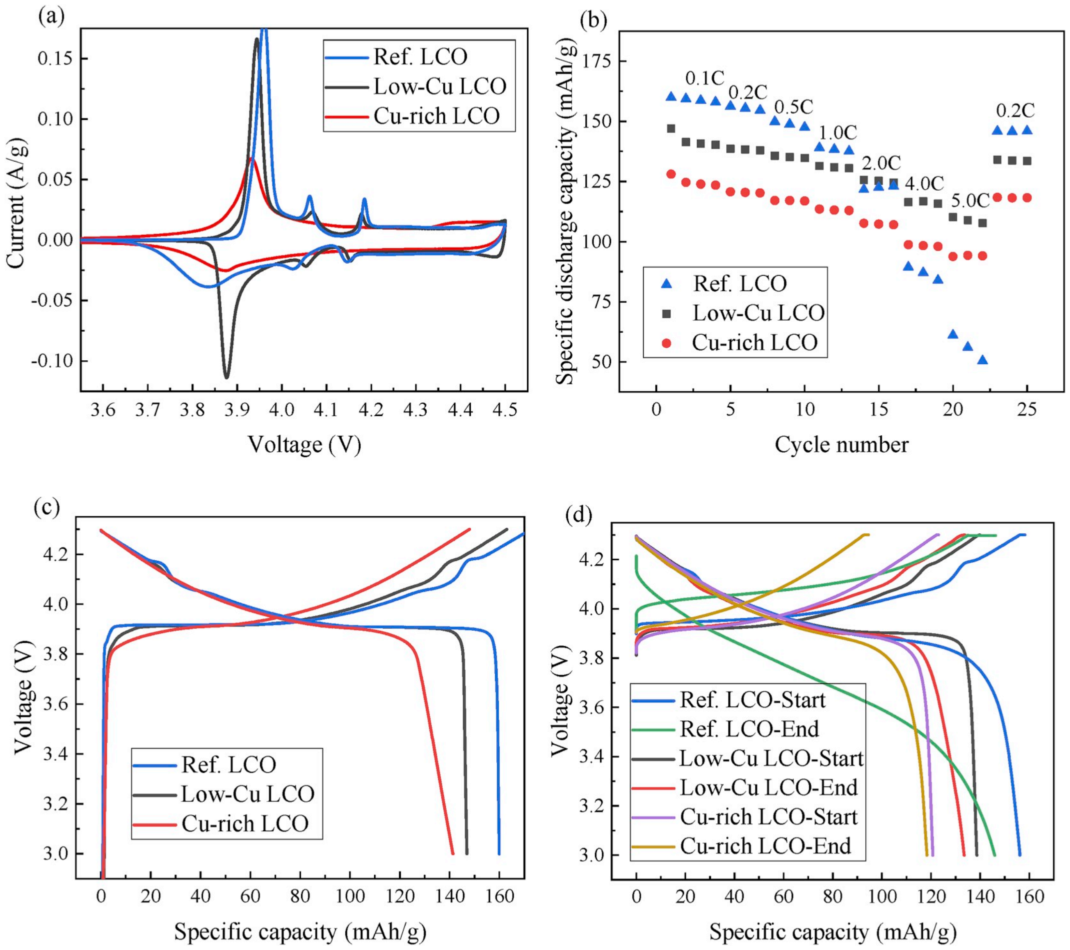

Fig. 4. The rate capability test results. a) cyclic voltammograms of the investigated materials, b) Specific capacity vs C-rate, c) Initial charge-discharge curves of the compared LCO samples (0.03C) and d) Charge-discharge curves of the cycled with 0.2 C at the beginning and at the end of the measurement.

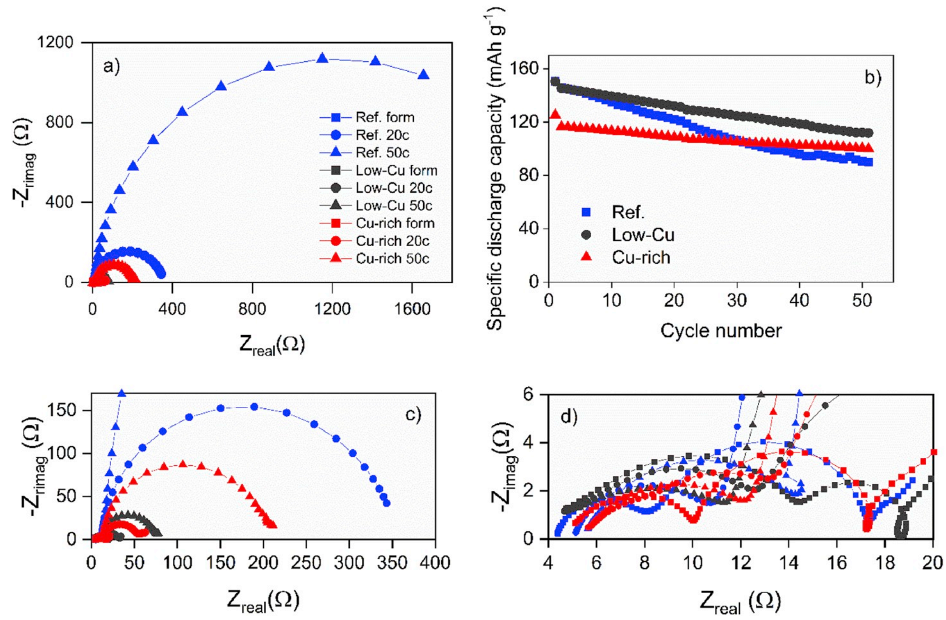

Fig. 5. The cycling and EIS results of the investigated materials. The Nyquist plots of the materials are presented in plots a), c) and d) in different scales, and the 0.5 C cycling results in plot b).

waste LIBs. Additionally, the influence of Cu on the electrochemical performance of the recycled active materials was investigated. A detailed mass balance of Li, Co and Cu during a typical hydrometallurgical recycling process was provided and it was found that levels of Li and Co recovery were only ca. 55% and 89%, respectively. Li was mainly lost in the solvent extraction and evaporation processes, whereas for Co, this occurred in the neutralization-precipitation stage. Moreover, the residual Cu present was extracted together with Co during solvent extraction, resulting in a contaminated $CoSO_4$ product.

The presence of copper contamination in the recycled cobalt salt and its subsequent inclusion into the LCO material causes a decrease in the initial specific capacity of the $LiCoO_2$ active materials. Nevertheless, the rate capability properties at high C-rates of 4.0 C or 5.0 C, was found to be higher for the Cu-contaminated active materials when compared to the virgin reference material. This can be explained by the better conductivity of the Cu containing LCOs, which decreases the over potentials during cycling, which gives rise to an increased capacity. The results highlight the contrary role of copper in battery recycling as it has offers both disadvantageous and advantageous behavior for recycled battery materials.

Declaration of competing interest

The authors declare that they have no known competing financial interests or personal relationships that could have appeared to influence the work reported in this paper.

Acknowledgements

This paper has been financially supported by the Strategic Research Council of the Academy of Finland (Closeloop project, grant number 303454). The authors also like to acknowledge the collaboration with Business Finland supported projects (CMEco and BATCircle, grant numbers ln7405/31/2016 and 4853/31/2018) and the additional financial support from the Chinese Scholarship Council. Special thanks also go to AkkuSer Ltd for providing the spent battery waste used in this study. This research also made use of the RawMatters Infrastructure (RAMI) based at Aalto University and funded by the Academy of Finland.

Appendix A. Supplementary data

Supplementary data to this article can be found online at https://doi.org/10.1016/j.jpowsour.2019.227630.

References

[1] J.B. Goodenough, K.-S. Park, The Li-ion rechargeable battery: a perspective, J. Am. Chem. Soc. 135 (2013) 1167–1176.

[2] E.M. Sarkar, T. Sarkar, M.D. Bharadwaj, Lithium-ion battery supply chain: enabling national electric vehicle and renewables targets, Curr. Sci. 114 (2018) 2453–2458.

[3] C. Xu, W. Zhang, W. He, G. Li, J. Huang, H. Zhu, Generation and management of waste electric vehicle batteries in China, Environ. Sci. Pollut. Res. 24 (2017) 20825–20830.

[4] X. Zeng, J. Li, N. Singh, Recycling of spent lithium-ion battery: a critical review, Crit. Rev. Environ. Sci. Technol. 44 (2014) 1129–1165.

[5] E.G. Thomas, Recycling Rates of Metals: A Status Report, United Nations Environment Programme, 2011.

[6] B. Swain, Recovery and recycling of lithium: a review, Separ. Purif. Technol. 172 (2017) 388–403.

[7] Hans Eric Melin, State-of-the-art in Reuse and Recycling of Lithium-Ion Batteries – A Research Review, 2019.

[8] W. Gao, C. Liu, H. Cao, X. Zheng, X. Lin, H. Wang, Y. Zhang, Z. Sun, Comprehensive evaluation on effective leaching of critical metals from spent lithium-ion batteries, Waste Manag. 75 (2018) 477–485.

[9] B. Huang, Z. Pan, X. Su, L. An, Recycling of lithium-ion batteries: recent advances and perspectives, J. Power Sources 399 (2018) 274–286.

[10] L. Li, X. Zhang, M. Li, R. Chen, F. Wu, K. Amine, J. Lu, The recycling of spent lithium-ion batteries: a review of current processes and technologies, Electrochem. Energy Rev. 1 (2018) 461–482.

[11] L. Li, W. Qu, X. Zhang, J. Lu, R. Chen, F. Wu, K. Amine, Succinic acid-based leaching system: a sustainable process for recovery of valuable metals from spent Li-ion batteries, J. Power Sources 282 (2015) 544–551.

[12] C. Peng, F. Liu, A.T. Aji, B.P. Wilson, M. Lundström, Extraction of Li and Co from industrially produced Li-ion battery waste – using the reductive power of waste itself, Waste Manag. 95 (2019) 604–611.

[13] C.-H. Jo, S.-T. Myung, Efficient recycling of valuable resources from discarded lithium-ion batteries, J. Power Sources 426 (2019) 259–265.

[14] X. Chen, B. Xu, T. Zhou, D. Liu, H. Hu, S. Fan, Separation and recovery of metal values from leaching liquor of mixed-type of spent lithium-ion batteries, Separ. Purif. Technol. 144 (2015) 197–205.

[15] L. Chen, X. Tang, Y. Zhang, L. Li, Z. Zeng, Y. Zhang, Process for the recovery of cobalt oxalate from spent lithium-ion batteries, Hydrometallurgy 108 (2011) 80–86.

[16] L. Sun, K. Qiu, Vacuum pyrolysis and hydrometallurgical process for the recovery of valuable metals from spent lithium-ion batteries, J. Hazard Mater. 194 (2011) 378–384.

[17] J. Kang, G. Senanayake, J. Sohn, S.M. Shin, Recovery of cobalt sulfate from spent lithium ion batteries by reductive leaching and solvent extraction with Cyanex 272, Hydrometallurgy 100 (2010) 168–171.

[18] C. Peng, F. Liu, Z. Wang, B.P. Wilson, M. Lundström, Selective extraction of lithium (Li) and preparation of battery grade lithium carbonate (Li_2CO_3) from spent Li-ion batteries in nitrate system, J. Power Sources 415 (2019) 179–188.

[19] X. Chen, Y. Chen, T. Zhou, D. Liu, H. Hu, S. Fan, Hydrometallurgical recovery of metal values from sulfuric acid leaching liquor of spent lithium-ion batteries, Waste Manag. 38 (2015) 349–356.

[20] V. Sridhar, J.K. Verma, Extraction of copper, nickel and cobalt from the leach liquor of manganese-bearing sea nodules using LIX 984N and ACORGA M5640, Miner. Eng. 24 (2011) 959–962.

[21] S. Shi, C. Ouyang, M. Lei, W. Tang, Effect of Mg-doping on the structural and electronic properties of $LiCoO_2$: a first-principles investigation, J. Power Sources 171 (2007) 908–912.

[22] S.A. Needham, G.X. Wang, H.K. Liu, V.A. Drozd, R.S. Liu, Synthesis and electrochemical performance of doped $LiCoO_2$ materials, J. Power Sources 174 (2007) 828–831.

[23] J. Kim, H. Kang, N. Go, S. Jeong, T. Yim, Y. Nam Jo, K. Tae Lee, J. Mun, Egg-shell structured $LiCoO_2$ by Cu^{2+} substitution to Li^+ sites via facile stirring in an aqueous copper(ii) nitrate solution, J. Mater. Chem. A. 5 (2017) 24892–24900.

[24] C. Nithya, R. Thirunakaran, A. Sivashanmugam, S. Gopukumar, Microwave synthesis of novel high voltage (4.6V) high capacity $LiCu_xCo_{1-x}O_{2\pm\delta}$ cathode material for lithium rechargeable cells, J. Power Sources 196 (2011) 6788–6793.

[25] C. Nithya, R. Thirunakaran, A. Sivashanmugam, S. Gopukumar, High-performing $LiMg_xCu_yCo_{1-x-y}O_2$ cathode material for lithium rechargeable batteries, ACS Appl. Mater. Interfaces 4 (2012) 4040–4046.

[26] R. Thirunakaran, T. Kim, W. Yoon, Synthesis and electrochemical characterization on dual-doped $LiCoO_2$ via green chemistry method for lithium rechargeable batteries, J. Appl. Electrochem. 44 (2014) 709–718.

[27] K. Kang, G. Ceder, Factors that affect Li mobility in layered lithium transition metal oxides, Phys. Rev. B. 74 (2006), 094105.

[28] N. Vieceli, C.A. Nogueira, C. Guimarães, M.F. Pereira, F.O. Durão, F. Margarido, Hydrometallurgical recycling of lithium-ion batteries by reductive leaching with sodium metabisulphite, Waste Manag. 71 (2018) 350–361.

[29] C. Peng, J. Hamuyuni, B.P. Wilson, M. Lundström, Selective reductive leaching of cobalt and lithium from industrially crushed waste Li-ion batteries in sulfuric acid system, Waste Manag. 76 (2018) 582–590.

[30] D. Dutta, A. Kumari, R. Panda, S. Jha, D. Gupta, S. Goel, M.K. Jha, Close loop separation process for the recovery of Co, Cu, Mn, Fe and Li from spent lithium-ion batteries, Separ. Purif. Technol. 200 (2018) 327–334.

[31] S. Virolainen, M. Fallah Fini, A. Laitinen, T. Sainio, Solvent extraction fractionation of Li-ion battery leachate containing Li, Ni, and Co, Separ. Purif. Technol. 179 (2017) 274–282.

[32] J. Pudas, A. Erkkila, J. Viljamaa, Battery Recycling Method, US8979006B2, 2015.

[33] J. Nan, D. Han, X. Zuo, Recovery of metal values from spent lithium-ion batteries with chemical deposition and solvent extraction, J. Power Sources 152 (2005) 278–284.

[34] T. Ohzuku, A. Ueda, Solid-state redox reactions of $LiCoO_2$ ($R\bar{3}m$) for 4 volt secondary lithium cells, J. Electrochem. Soc. 141 (1994) 2972–2977.

[35] J.N. Reimers, J.R. Dahn, Electrochemical and in situ X-ray diffraction studies of lithium intercalation in Li_xCoO_2, J. Electrochem. Soc. 139 (1992) 2091–2097.

[36] J.N. Reimers, J.R. Dahn, U. von Sacken, Effects of impurities on the electrochemical properties of $LiCoO_2$, J. Electrochem. Soc. 140 (1993) 2752–2754.

[37] D. Andre, M. Meiler, K. Steiner, C. Wimmer, T. Soczka-Guth, D.U. Sauer, Characterization of high-power lithium-ion batteries by electrochemical impedance spectroscopy. I. Experimental investigation, J. Power Sources 196 (2011) 5334–5341.

[38] J. Li, E. Murphy, J. Winnick, P.A. Kohl, Studies on the cycle life of commercial lithium ion batteries during rapid charge – discharge cycling, J. Power Sources 102 (2001) 294–301.